Magnetic-sublevel population and alignment for the excitation of H- and He-like uranium in relativistic collisions

A. Gumberidze,[1,2] S. Fritzsche,[2,3,4] S. Hagmann,[3,7] C. Kozhuharov,[3] X. Ma,[8] M. Steck,[3] A. Surzhykov,[3,5]
A. Warczak,[6] and Th. Stöhlker[3,5,9]

[1]*ExtreMe Matter Institute EMMI and Research Division, GSI Helmholtzzentrum für Schwerionenforschung, D-64291 Darmstadt, Germany*
[2]*FIAS Frankfurt Institute for Advanced Studies, D-60438 Frankfurt am Main, Germany*
[3]*GSI Helmholtzzentrum für Schwerionenforschung, D-64291 Darmstadt, Germany*
[4]*Department of Physics, University of Oulu, P.O. Box 3000, FIN-90014, Finland*
[5]*Physikalisches Institut, Ruprecht-Karls-Universität, Heidelberg, Germany*
[6]*Institute of Physics, Jagiellonian University, Krakow, Poland*
[7]*Institut für Kernphysik, University of Frankfurt, D-60486 Frankfurt, Germany*
[8]*Institute of Modern Physics, 730000 Lanzhou, China*
[9]*Helmholtz-Institut Jena, D-07743 Jena, Germany*

We have measured the alignment of the L-shell magnetic substates following the K-shell excitation of hydrogen- and helium-like uranium in relativistic collisions with a low-Z gaseous target. Within this experiment, the population distribution for the L-shell magnetic sublevels has been obtained via an angular differential study of the decay photons associated with the subsequent deexcitation process. The results show a very distinctive behavior for the H- and He-like heavy systems. In particular, for $K \to L$ excitation of He-like uranium, a considerable alignment of the L-shell levels was observed. A comparison of our experimental findings with recent rigorous relativistic predictions provides a good qualitative and a reasonable quantitative agreement, emphasizing the importance of the magnetic-interaction and many-body effects in the strong-field domain of high-Z ions.

PACS number(s): 34.50.Fa, 32.30.Rj

I. INTRODUCTION

Relativistic collisions involving heavy high-Z ions provide an opportunity for comprehensive testing of our understanding of elementary processes related to ultrafast electromagnetic interactions and serve thus as an important testing ground for fundamental atomic theories. One of the elementary processes is the ionization of a strongly bound projectile electron caused by the Coulomb interaction with the target nucleus. For relativistic [1] and even ultrarelativistic collisions [2], this process has been the subject of intense experimental and theoretical studies over many years where the validity of perturbation theory, the proper choice of wave function, and the relevance of the magnetic part of the interaction were in the focus of the investigations (see [1–11] and references therein). Very recently, K-shell ionization has attracted particular attention as a tool for atomic structure investigation [12], since for few-electron ions this process exhibits an extraordinary state selectivity [13]. In general, an overall agreement between experimental data and refined theoretical treatments can be stated, but there is still an indication of a small but systematic deviation between experiment and theory for very asymmetric collision systems [10,11] where first-order perturbation theory is expected to be an excellent approximation.

Compared to ionization, Coulomb excitation is mediated by the same interaction mechanism, but the projectile electron is excited into a bound state of the ion and not into the continuum. Therefore, a much better experimental control can be expected by measuring the deexcitation photons. Earlier experimental and theoretical studies for high-Z have focused on total cross sections for K-shell electron excitation by using H- and He-like Bi and H-like Au projectiles [14–17]. The

results obtained have shown, in particular, the importance of the magnetic part of the Lienard-Wiechert interaction, namely the need to include the magnetic term coherently into the excitation amplitude, leading to reduced total excitation cross sections. This coherent incorporation of the electric and magnetic parts of the interaction potential is in contrast to any quasirelativistic approach in which these contributions are added incoherently and which has been applied quite successfully for the description of the ionization process. In Ref. [18], simultaneous excitation and ionization of He-like uranium has been addressed. The obtained experimental cross sections when compared to relativistic calculations based on the independent particle approximation and first-order perturbation theory have provided reasonable agreement for lighter targets, whereas for heavy targets systematic deviations have been observed. In [19], a relativistic symmetric eikonal model was applied for the description of this process, which provided significantly better agreement with the experimental results.

Compared to total cross sections, differential measurements often provide more detailed insights into the mechanism of a particular process [20]. As an example, for radiative electron capture (REC) into high-Z ions, former investigations of angular differential photon emission and alignment of the associated excited states gave access to many subtle details of relativistic atomic collision dynamics as well as of the electronic structure of high-Z ions [21–23]. In addition, we like to note that the alignment and polarization phenomena in ion-atom collisions have been studied in several earlier investigations, in particular for low-Z ions (see, for example [24–27]). The K-shell x-ray radiation produced by electron

capture (and in a few cases via excitation) in few-electron ions from target atoms has been found to be anisotropic and the corresponding orientation and alignment parameters have been obtained by measuring the x-ray polarization or angular differential cross sections [24–27]. However, in those studies, mainly low-Z ions in the relatively low collision energy regime have been investigated. Besides, in most of the cases it has not been possible to unambiguously resolve individual transitions contributing to the observed x-ray lines.

In this paper, we present an experimental study of the angular differential photon emission following the K-shell excitation of the heaviest H- and He-like systems in relativistic collisions with N_2 molecules. From the angular-resolved measurement of the x-ray emission following K-shell excitation, we were able to determine the associated population distributions for the magnetic L-shell sublevels belonging to the $2p_{3/2}$ state in H-like uranium and to the $^1P_1$ and $^3P_1$ states in He-like uranium, respectively. The results display a very different behavior for the two (hydrogen- and helium-like) systems under consideration, contradicting the usual viewpoint that the coupling of the electrons and their interaction only plays a minor role in the high-Z regime.

The paper is structured as follows. In the next section, the experimental arrangement as well as the experimental method is described; in Sec. III, we then present the data analysis and compare our experimental results for subshell- and angular-differential cross sections with the predictions of a fully relativistic theory. In Sec. IV, finally, a short summary and conclusions are given.

II. EXPERIMENTAL ARRANGEMENT

Experimental information about Coulomb excitation of one- and few-electron projectiles occurring in relativistic atomic collisions is very scarce. The lack of data arises mainly from experimental difficulties due to the fact that excitation is not accompanied by a projectile charge exchange. As a consequence, this process can usually only be studied in single-pass experiments by measuring the photon production in coincidence with primary beams of low intensity [14,18]. Recently, an alternative experimental approach has been introduced at the Experimental Storage Ring (ESR) at GSI, where projectile excitation has been studied by detecting the projectile x-ray emission in anticoincidence with charge exchange [17,28]. In our study, we have utilized this technique to extend the earlier investigations to a more detailed analysis of the Coulomb excitation of U^{91+}, U^{90+}, and their angular-differential x-ray emission in relativistic collisions with a N_2 target.

The experiment was performed at the ESR by using H- and He-like uranium ions delivered by the heavy ion synchrotron (SIS) at an energy of 217 MeV/u. An efficient electron cooling in the ESR storage ring provided beams with very low emittance (beam size of less than 5 mm) and a longitudinal momentum spread of $\Delta p/p \sim 10^{-5}$, which enabled storage of the beam with long lifetimes as well as a decrease of the uncertainties due to the relativistic Doppler effect. After injection in the ring and following cooling, the ion beam interacted with a supersonic jet of N_2 target. For the experiment, the atomic physics photon detection chamber of

the internal target of the ESR was utilized. Here, projectile x-rays produced in collisions of the stored ion beams with the jet target were detected by an array of solid-state detectors, covering observation angles in the range between $10°$ and $150°$ with respect to the beam axis. The Ge(i) photon detectors were energy and efficiency calibrated before the experiment using a set of appropriate radioactive sources. In addition, those projectile ions that captured an electron were detected after the next dipole magnet of the ESR with a multiwire proportional counter (MWPC). A detailed description of the detection setup at the ESR jet target and of the utilized anticoincidence technique can be found in [17,29] and in references therein.

As an example, we depict in Fig. 1 x-ray spectra recorded for $U^{91+} \rightarrow N_2$ collisions at the forward angle of close to $10°$. In the total spectra (a), measured without any coincidence condition, the characteristic transitions arising from both
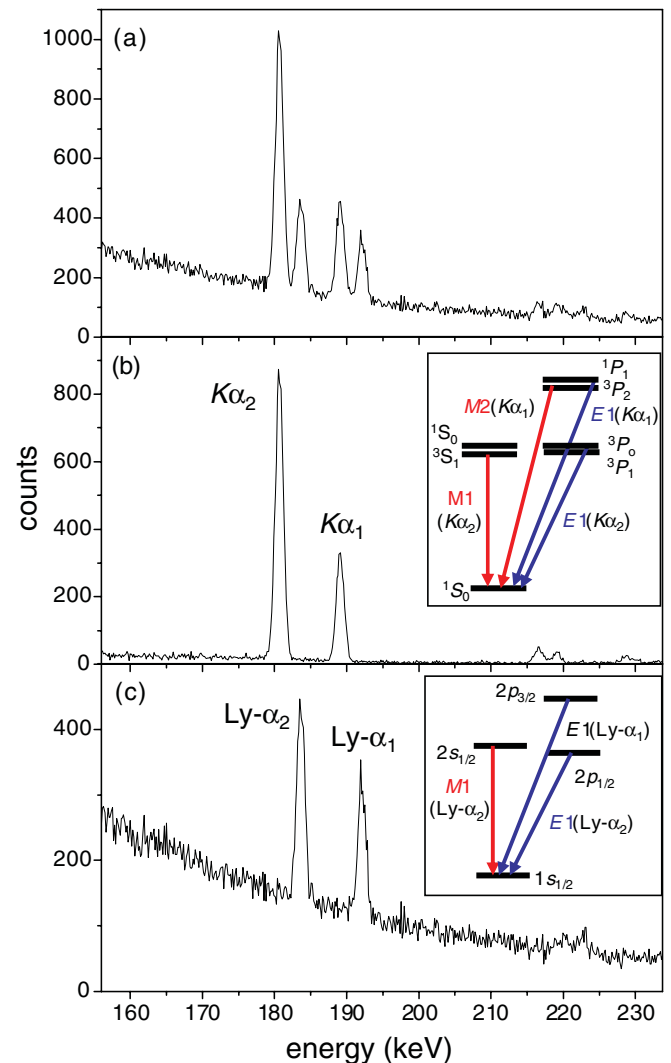

FIG. 1. (Color online) X-ray spectra recorded for 217 MeV/u $U^{91+} \rightarrow N_2$ collisions at the forward angle of close to $10°$: (a) total emission spectrum without coincidence requirement; (b) photons in coincidence with electron capture, $L \rightarrow K$ transitions in He-like uranium; (c) photons in anticoincidence with electron capture, $L \rightarrow K$ transitions in H-like uranium. The insets show the corresponding level schemes and transitions.

electron capture ($K\alpha$ transitions in He-like uranium) and from excitation (Ly-α transitions in H-like uranium) are clearly visible. Applying a coincidence requirement with the down-charged projectile, we obtain the characteristic x-ray spectra corresponding exclusively to the events of capture of one electron from the N_2 into initially H-like uranium (U^{91+}). Furthermore, by substraction of the spectrum corresponding to a capture (b) from the total one (a), we obtain the spectrum in anticoincidence with the projectile charge exchange (c), which comprises only the events corresponding to $K \rightarrow L$ excitation (and following decay) of the projectile electron. Indeed, no He-like $K\alpha$ transitions are observed in the anticoincidence spectrum. This also proves that the MWPC detector used for particle detection operates with a detection efficiency very close to 100%. The exponential background observed in the excitation spectrum stems from electron bremsstrahlung. In the same way, a spectrum containing only the events corresponding to $K \rightarrow L$ excitation has also been obtained for He-like projectiles. In this case, the situation is even more favorable because K-shell transitions can only be produced by a K-shell excitation.

Finally, we like to note that the data for initially H- and He-like uranium have been acquired with an identical detector setup in sequential order during the same beam time. The ion beam position was defined by the target in both cases and, thus, stayed unchanged. Therefore, the detector geometry with respect to the beam axis was the same for both beams. This is very important, since it allows us to normalize the observed yields of x-ray transitions in He-like ions to the line intensity of Ly-α_1 transition, which is known to be precisely isotropic (see below).

III. DATA ANALYSIS AND RESULTS

In the following, we focus on the angular distributions of characteristic x rays following the excitation of H- and He-like projectiles. Such an angle-resolved analysis will enable us to gain insight into a mechanism of formation of excited ionic substates in relativistic ion-atom collisions. The information on the magnetic sublevel population of the excited ion can be directly extracted from the angular distribution of deexcitation photons that can be written in the projectile (emitter) frame as

$$W(\theta) = A_0 + A_2 P_2(\cos\theta) \propto 1 + \beta_{20}\left(1 - \tfrac{3}{2}\sin^2\theta\right). \quad (1)$$

Here, θ is the angle between the direction of the deexcitation photon and the beam direction, while P_2 denotes the second-order Legendre polynomial.

The emission pattern (1) is completely determined by the effective anisotropy parameter β_{20}, whose particular form depends on the transition under consideration. For example, for the Ly-α_1 ($2p_{3/2} \rightarrow 1s_{1/2}$) decay in H-like ions, the anisotropy $\beta_{20} = \mathcal{A}_2 f(E1,M2)/2$ includes the alignment parameter,

$$\mathcal{A}_2 = \frac{\sigma\left(\tfrac{3}{2}, \pm\tfrac{3}{2}\right) - \sigma\left(\tfrac{3}{2}, \pm\tfrac{1}{2}\right)}{\sigma\left(\tfrac{3}{2}, \pm\tfrac{3}{2}\right) + \sigma\left(\tfrac{3}{2}, \pm\tfrac{1}{2}\right)}, \quad (2)$$

which can be written in terms of the partial cross sections $\sigma(j\mu)$ for populating the magnetic substates $|j\mu\rangle$, and the so-called structure function $f(E1,M2)$ [23]. This function describes the interference between the leading $E1$ and the

much weaker $M2$ decay channels and contributes by as much as $f(E1,M2) = 1.28$ to the angular distribution of the characteristic photon emission from H-like uranium ions. In contrast to the Ly-α_1 transition, no multipole mixing can occur for the decay of the $[1s,2p_{1/2}]\,^3P_1$ and $[1s,2p_{3/2}]\,^1P_1$ states in He-like ions, since they can only decay via a fast $E1$ transition to the ground state. For the $K\alpha_1$ ($2\,^1P_1 \rightarrow 1\,^1S_0$) and $K\alpha_2$ ($2\,^3P_1 \rightarrow 1\,^1S_0$) transitions, therefore, the angular distribution (1) is governed by the anisotropy parameter $\beta_{20} = \mathcal{A}_2/\sqrt{2}$, where the alignment parameter reads

$$\mathcal{A}_2 = \sqrt{2}\frac{\sigma(1, \pm 1) - \sigma(1,0)}{2\sigma(1, \pm 1) + \sigma(1,0)}. \quad (3)$$

Here, the partial cross sections $\sigma(J,M)$ describe the dynamics of excitation of the two-electron projectiles [30].

In our experiment, we strongly benefit from the fact that the Ly-α_2 transition arising from the decay of the $2s_{1/2}$ and $2p_{1/2}$ levels is known to be precisely isotropic. Consequently, this line provides an ideal tool to measure a possible anisotropy of the close-spaced Ly-α_1 or $K\alpha$ transitions. By using this transition for normalization purposes, various systematic effects, associated for example with solid angle corrections, possible error in detector efficiency calibration, etc., cancel out. This technique has been successfully applied in previous studies [22]. In Fig. 2, the result for the emission pattern of the Ly-α_1 ($2p_{3/2} \rightarrow 1s_{1/2}$) transition is shown, normalized to the Ly-α_2 intensity. The angular distribution is fairly isotropic. From this experimental result, we extract the value of the alignment parameter for the $2p_{3/2}$ state by fitting Eq. (1) (transformed into the laboratory frame) to the observed angular distributions (see Fig. 2). The anisotropy coefficient β_{20} and an overall amplitude of the fit function were kept as free fit parameters. From this procedure, we obtained a value of 0.013 ± 0.086 for the alignment $\mathcal{A}_2$ that is consistent with the isotropic angular distribution. The quoted uncertainty is entirely of statistical origin. This finding is in agreement with theoretical predictions (see Fig. 4) showing no alignment for the particular collision energy used in the experiment. Here, we like to note that this result is markedly different to earlier findings obtained for the same transition in U^{91+} ($2p_{3/2} \rightarrow 1s_{1/2}$) but caused by REC (the same beam energy and the same target) [22,23], where a very strong alignment
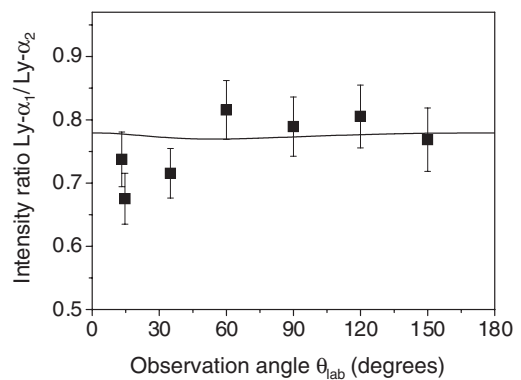

FIG. 2. Intensity of Ly-α_1 transition normalized to the Ly-α_2 line intensity as a function of observation angle for 217 MeV/u $U^{91+} \rightarrow N_2$ collisions. The solid line refers to a fit of Eq. (1) (transformed into the laboratory frame) to the data.
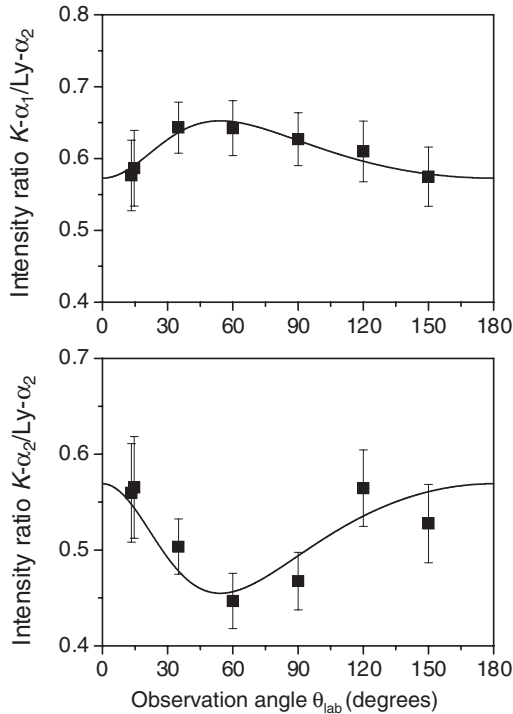
FIG. 3. Angular distributions of $K\alpha_1$ (top part) and $K\alpha_2$ (bottom part) measured for K-shell excitation of He-like uranium in collisions with N_2 at 217 MeV/u. In addition, fits of Eq. (1) (transformed into the laboratory frame) to the corresponding experimental data are shown by solid lines.

has been observed. Moreover, in our experiment, we observed a very different behavior for the K-shell excitation of He-like uranium as compared to the H-like case. In Fig. 3, the $K\alpha_1$ and $K\alpha_2$ angular distributions as measured for K-shell excitation of He-like uranium in 217 MeV/u $U^{90+} \rightarrow N_2$ collisions are presented, normalized to the Ly-α_2 yield as obtained for H-like uranium. As seen from the figure, the data [especially $K\alpha_2$ ($[1s_{1/2}, 2p_{1/2}]^3P_1 \rightarrow 1\,^1S_0$)] exhibit a pronounced deviation from a constant intensity ratio.

Let us note here, moreover, that for the case of K-shell excitation of high-Z He-like ions, only the $[1s_{1/2}, 2p_{3/2}]^1P_1$ and the $[1s_{1/2}, 2p_{1/2}]^3P_1$ states are predicted to be populated and contribute to the observed $K\alpha_1$ and $K\alpha_2$ transitions [30]. In both cases, an alignment of the different sublevels is possible. As is seen from Fig. 3, there is a significant positive alignment for the $[1s_{1/2}, 2p_{1/2}]^3P_1$ level ($K\alpha_2$ transition) and a negative alignment for the $[1s_{1/2}, 2p_{3/2}]^1P_1$ state ($K\alpha_1$ transition). Applying the same procedure as for the case of the H-like ions (described above), we obtained values of -0.12 ± 0.07 and 0.22 ± 0.08 for the alignment parameters of the $^1P_1$ and $^3P_1$ states, respectively. The quoted uncertainties are entirely of statistical origin.

We can compare these experimental results with values of -0.172 and $+0.110$ given by recent fully relativistic calculations [30,31]. In these computations, both the coupling of the electrons as well as their repulsive interaction have been taken into account within the framework of the multiconfiguration Dirac-Fock method (MCDF). These calculations included, moreover, the cascade feeding (following an initial excitation into states with $n \geqslant 3$) and its effect upon the alignment of the $^1P_1$ and $^3P_1$ states, in addition to the alignment as obtained for a direct $K \rightarrow L$ excitation. As known from photoinduced excitation of atoms and ions [32], the different sign in the alignment of the $^1P_1$ and $^3P_1$ states arises from the different coupling of the two electrons. Though the alignment differs quite considerably for these two states, it may be both negative (low projectile energies) or positive (high projectile energies) as seen from Fig. 4. Let us note that this qualitative behavior of the alignment as a function of energy has been already predicted by earlier nonrelativistic calculations for $^1S_0 \rightarrow\,^1P_1$ excitation [33–35] and it holds true also for excitation of H-like systems ($1s_{1/2} \rightarrow 2p_{3/2}$) [14]. This finding is simply related to the fact that with increasing energy more angular momentum is transferred to the system so that transitions with $\Delta m = \pm 1$ (He-like system) start to dominate [14,16,30]. From the comparison in Fig. 4, a very good agreement with the experimental result for the alignment of the $^1P_1$ state can be seen. For the $^3P_1$ level, the theoretical value is smaller than the experimental one; however, the deviation is not particularly
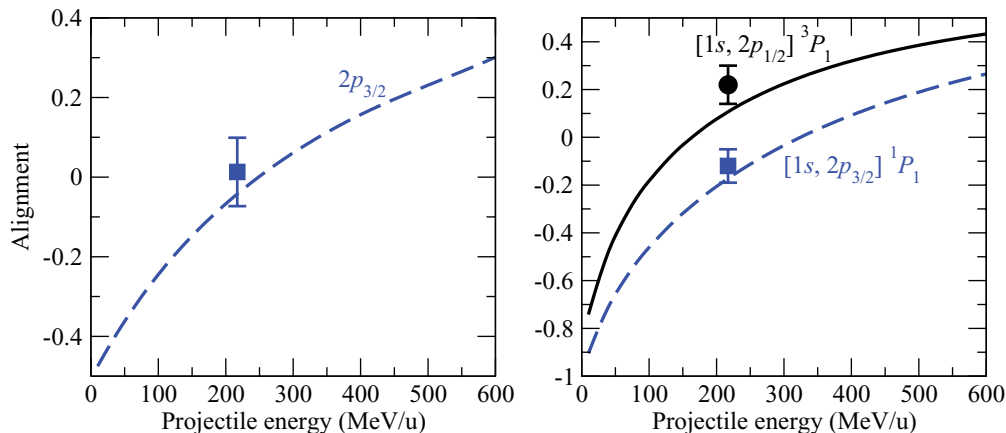

FIG. 4. (Color online) Alignment parameters A_2 of the $2p_{3/2}$ state of hydrogen-like (left panel) and the $[1s_{1/2}, 2p_{1/2}]^3P_1$ as well as the $[1s_{1/2}, 2p_{3/2}]^1P_1$ states of helium-like (right panel) uranium ions following K-shell excitation. Results of relativistic calculations are compared with the experimental findings for collisions with the N_2 target at the energy of 217 MeV/u.

pronounced due to the experimental uncertainty. Here it is important to note that the theoretical values include only the Coulomb excitation due to the target nucleus and omit completely the process of electron impact excitation. Coulomb excitation caused by the nuclear charge Z_T of the target scales with Z_T^2, whereas the cross section for electron impact excitation scales linearly with the amount of target electrons available. Therefore, for the particular case of nitrogen target, we might expect that electron impact excitation contributes by about 15% to the overall excitation cross section.

IV. SUMMARY AND OUTLOOK

In summary, we have performed the first experimental study of the magnetic-sublevel population for the K-shell excitation of hydrogen- and helium-like uranium in relativistic collisions with a low-Z gaseous target. The information about the population of the magnetic sublevels in this process has been obtained via an angular differential study of the decay photons associated with Coulomb excitation. The results presented in this work show a markedly different behavior for the different ion species (H-like or He-like). The Lyman transition $(2p_{3/2} \rightarrow 1s_{1/2})$ following K-shell excitation of H-like uranium has been found to be nearly isotropic and therefore the population of the magnetic sublevels follows a statistical distribution. For the $K \rightarrow L$ excitation of He-like uranium, in contrast, we have measured an nonzero alignment for both $^3P_1$ and $^1P_1$ states, but with alignment parameters of opposite sign. Though perhaps not very surprising in its own, this result cannot be understood just within a single-electron

model but requires one to account for the coupling of the electrons as well as their interaction. This is remarkable as we are dealing with high-Z ions for which the interaction among the electrons is commonly assumed to be of minor importance. The experimental data agree well with recent theoretical predictions [30] in which both the relativistic and magnetic interaction effects were taken into account and thus provide a meaningful description of the K-shell excitation process in relativistic collisions of high-Z ions with low-Z targets. However, since this is the only measurement for H- and He-like uranium to date, additional studies with different targets and different collision energies would be desirable to unravel especially the role of electron impact excitation in collisions of high-Z ions with gaseous targets. Since the ESR storage ring provides uranium beams with energies from $\sim$10 MeV/u up to $\sim$ 400 MeV/u, we plan, as a next step, to perform measurements at a few different energies in this range. These investigations will be supported additionally by the observation of linear polarization of the deexcitation x rays as very recently introduced in experiments at the ESR [36].

[1] J. Eichler and W. Meyerhof, *Relativistic Atomic Collisions* (Academic Press, New York, 1995).

[2] A. Belkacem, H. Gould, B. Feinberg, R. Bossingham, and W. E. Meyerhof, Phys. Rev. A **56**, 2806 (1997).

[3] A. Belkacem, N. Claytor, T. Dinneen, B. Feinberg, and H. Gould, Phys. Rev. A **58**, 1253 (1998).

[4] H. F. Krause, C. R. Vane, S. Datz, P. Grafström, H. Knudsen, C. Scheidenberger, and R. H. Schuch, Phys. Rev. Lett. **80**, 1190 (1998).

[5] N. Claytor, A. Belkacem, T. Dinneen, B. Feinberg, and H. Gould, Phys. Rev. A **55**, R842 (1997).

[6] H. F. Krause, C. R. Vane, S. Datz, P. Grafström, H. Knudsen, C. Scheidenberger, and R. H. Schuch, Phys. Rev. Lett. **80**, 1190 (1998).

[7] K. Momberger, A. Belkacem, and A. H. Sørensen, Phys. Rev. A **53**, 1605 (1996).

[8] D. C. Ionescu and A. Belkacem, Phys. Scr., T **80**, 128 (1999); see also D. C. Ionescu and A. Belkacem, Eur. Phys. J. D **18**, 301 (2002).

[9] S. Fritzsche and T. Stöhlker, Phys. Scr., T **92**, 311 (2001).

[10] P. Rymuza *et al.*, J. Phys. B **26**, L169 (1993).

[11] Th. Stöhlker *et al.*, Nucl. Instrum. Methods Phys. Res., Sect. B **124**, 160 (1997).

[12] S. Trotsenko *et al.*, Phys. Rev. Lett. **104**, 033001 (2010).

[13] J. Rzadkiewicz *et al.*, Phys. Rev. A **74**, 012511 (2006).

[14] Th. Stöhlker *et al.*, Phys. Rev. A **57**, 845 (1998).

[15] Th. Stöhlker *et al.*, Phys. Lett. A **238**, 43 (1998).

[16] D. C. Ionescu and Th. Stöhlker, Phys. Rev. A **67**, 022705 (2003).

[17] A. Gumberidze, S. Fritzsche, F. Bosch, D. C. Ionescu, A. Krämer, C. Kozhuharov, Z. Stachura, A. Surzhykov, A. Warczak, and Th. Stöhlker, Phys. Rev. A **82**, 052712 (2010).

[18] T. Ludziejewski *et al.*, Phys. Rev. A **61**, 052706 (2000).

[19] B. Najjari and A. B. Voitkiv, J. Phys. B **41**, 115202 (2008).

[20] X. Ma, Th. Stöhlker, F. Bosch, O. Brinzanescu, S. Fritzsche, C. Kozhuharov, T. Ludziejewski, P. H. Mokler, Z. Stachura, and A. Warczak, Phys. Rev. A **64**, 012704 (2001).

[21] J. Eichler and Th. Stöhlker, Phys. Rep. **439**, 1 (2007).

[22] Th. Stöhlker *et al.*, Phys. Rev. Lett. **79**, 3270 (1997).

[23] A. Surzhykov, S. Fritzsche, A. Gumberidze, and Th. Stöhlker, Phys. Rev. Lett. **88**, 153001 (2002).

[24] E. Horsdal Pedersen, S. J. Czuchlewski, M. D. Brown, L. D. Ellsworth, and J. R. Macdonald, Phys. Rev. A **11**, 1267 (1975).

[25] L. D. Ellsworth, B. L. Doyle, U. Schiebel, and J. R. Macdonald, Phys. Rev. A **19**, 943 (1979).

[26] D. A. Church, R. A. Kenefick, D.-W. Wang, and R. L. Watson, Phys. Rev. A **26**, 3093 (1982).

[27] J. Palinkas, G. J. Pedrazzini, D. A. Church, R. A. Kenefick, C. A. Fulton, R. L. Watson, and D.-W. Wang, Phys. Rev. A **31**, 598 (1985).

[28] A. Krämer, Th. Stöhlker, S. Fritzsche, F. Bosch, D. Ionescu, C. Kozhuharov, T. Ludziejewski, P. Mokler, P. Rymuza, and Z. Stachura, Phys. Scr. **80**, 424 (1999).

[29] A. Gumberidze *et al.*, Hyperfine Interact. **146/147**, 133 (2003).

[30] A. Surzhykov, U. D. Jentschura, Th. Stöhlker, A. Gumberidze, and S. Fritzsche, Phys. Rev. A **77**, 042722 (2008).

[31] S. Fritzsche, J. Electron Spectrosc. Relat. Phenom. **114–116**, 1155 (2001).

[32] N. M. Kabachnik, S. Fritzsche, A. N. Grum-Grzhimailo, M. Meyer, and K. Ueda, Phys. Rep. **451**, 155 (2007).

[33] J. Van den Bos and F. J. De Heer, Physica **34**, 333 (1967).

[34] J. Van den Bos, Physica **42**, 245 (1969).

[35] F. Bell, J. Phys. B **17**, L65 (1984).

[36] G. Weber *et al.*, Phys. Rev. Lett. **105**, 243002 (2010).